Pak. J. Bot., 56(6): 2251-2264, 2024. DOI: http://dx.doi.org/10.30848/PJB2024-6(27)

APPLICATION OF ITS2 SECONDARY STRUCTURE IN SPECIES IDENTIFICATION AND CLASSIFICATION OF *REHMANNIA*

XIAORU CHENG[1 #], HAOYUAN LI[1 #], JIUCHANG SU[1,2], PEILEI CHEN[1,2], WANSHEN WANG[1], YOUSEF SULTAN[3] AND HONGYING DUAN[1,2*]

[1]College of Life Sciences, Henan Normal University, Xinxiang 453007, China
[2]Henan International Joint Laboratory of Aquatic Toxicology and Health Protection, College of Life Science, Henan Normal University, Xinxiang, Henan, 453007, China
[3]Department of Food Toxicology and Contaminants, National Research Centre, Dokki, Cairo 12622, Egypt
**Corresponding author's email: duanhy536@163.com*

Abstract

The internal transcribed spacer 2 (ITS2) sequence is known for its remarkable ability to distinguish between plant species, making it a valuable tool for phylogenetic analysis and species classification. In this investigation, we elucidated the secondary structure of ITS2 in *Rehmannia*, revealing a characteristic arrangement of four helices. It's noteworthy that the length and shape of each helix vary, contributing to significant interspecific differences. Furthermore, certain variants of *R. glutinosa* displayed notable disparities in their ITS2 secondary structures. Additionally, when comparing ITS2 sequences and secondary structures, we observed distinct differences between *Rehmannia* and its closely related genus, *Triaenophora*. This divergence highlighted the potential of ITS2, not only for genetic information but also for its structural characteristics, in enhancing species discrimination. Consequently, our findings underscore the substantial promise of ITS2 in the realms of species classification and identification.

Key words: *Rehmannia glutinosa*, DNA barcode, ITS2, Secondary structure.

Abbreviations: COI: Cytochrome c oxidase subunit I; ITS2: Internal transcribed spacer 2; *R.*: *Rehmannia*; K2P: Kimura two-parameter.

Introduction

The *Rehmannia* genus, categorized within Scrophulariaceae Sensu Lato, encompasses 6 distinct species: *R. glutinosa*, *R. piasezkii*, *R. elata*, *R. henryi*, *R. chingii* and *R. solanifolia*. Among these, the root of *R. glutinosa* is frequently employed for medicinal purposes and holds significant medicinal value, as highlighted by Duan *et al*., (2019). As a traditional Chinese herbal medicine, *R. glutinosa* boasts a lengthy history of both medicinal use and cultivation. It is characterized by its richness in glycosides, sugars, amino acids, and other vital components (Chen *et al*., 2021). Catalpol, a key bioactive compound in *R. glutinosa*, has been identified for its significant therapeutic properties. Studies by Huang *et al*., (2013) and Wang *et al*., (2015) suggest its potential in cancer prevention and enhancement of immune function. Additionally, research by Wang *et al*., (2013) underscores its capacity to resist aging and enhance hematopoietic abilities. Nevertheless, due to cross-pollination and seed preservation practices, the production process of *R. glutinosa* predominantly relies on asexual reproduction. This method leads to the coexistence of mixed *Rehmannia* species, posing challenges in both genetic breeding and quality identification of *Rehmannia*. Moreover, *R. piasezkii*, *R. elata*, and other *Rehmannia* species are frequently employed as substitutes for the medicinal herb Di Huang. This practice has implications for the quality of traditional Chinese herbal medicine Di Huang, as noted by Xia & Li (2009). Hence, precise classification and identification of specific *Rehmannia* species are crucial to guarantee the medicinal efficacy of traditional Chinese herbal medicine Di Huang.

DNA barcoding, a swiftly emerging method for species differentiation using concise DNA fragments, has gained prominence in biotaxonomy research (Shinwari *et al*., 1994; Duan *et al*., 2019). Given that the cytochrome c oxidase subunit I (*COI*) serves as a DNA barcode for animal identification (Hebert *et al*., 2003), it is currently extensively applied in discriminating and identifying various animals, including insects, fish, birds, and others. Nevertheless, the evolutionary pace of the *COI* gene is notably slower in plants, rendering it primarily suitable for the identification of certain algae species. In order to find the ideal plant DNA barcoding, researchers have actively explored both the chloroplast and nuclear genomes. Numerous barcode fragments or their combinations have been proposed (Shinwari *et al*., 1994a; Chase *et al*., 2007; Kress *et al*., 2005; Pennisi, 2007). Among these, *rbcL* and *matK* are recommended as core barcodes, while *trnH-psbA* and ITS are suggested as supplementary barcodes (Shinwari, 1995; Hollingsworth *et al*., 2009). Extensive comparisons and evaluations of the aforementioned candidate DNA barcodes have revealed that the combination of *trnH-psbA* and ITS demonstrates efficacy in species identification within *Betulaceae*, *Malvaceae*, *Panax*, *Parnassia*, and other taxa (Ren *et al*., 2010; Zuo *et al*., 2011; Yang *et al*., 2012).

Additionally, certain studies have highlighted the effectiveness of ITS2 in plant species identification, with a success rate ranging from 78% to 100% in the identification of species within *Rosaceae*, *Leguminosae*, *Euphorbia*, *Rutaceae*, *Paris*, *Compositae*, and other families (Shinwari, 1998; Luo *et al*., 2010; Chen *et al*., 2010; Gao *et al*., 2011). Chen *et al*., (2010) conducted an analysis of ITS2 sequences from 4800 medicinal plants across 753 genera. Their

findings revealed a remarkable species-level identification efficiency of 92.7% for ITS2 (Chen *et al*., 2010). Furthermore, ITS2 demonstrated successful identification of certain medicinal materials and counterfeits in studies conducted by Liu *et al*., (2012), Luo *et al*., (2012), and Peng *et al*., (2012). In conclusion, DNA barcoding proves to be a straightforward and efficient method, unencumbered by the morphological constraints of samples, and has demonstrated accurate identification of Chinese medicinal materials (Shinnwari, 2000; Ren *et al*., 2010).

To establish DNA barcodes for a vast array of Chinese herbal medicines, the State Pharmacopoeia Commission devised the "Guiding Principles for DNA Barcode Molecular Identification of Chinese Medicinal Herbs." This initiative led to the establishment of a plant DNA barcode identification system based on ITS2 and *trnH-psbA* (Chinese Pharmacopoeia, 2015). This study undertakes an analysis of ITS2 sequences within the *Rehmannia* and *Triaenophora* genera, with a specific emphasis on their composition and secondary structure. The findings contribute to a theoretical framework supporting the application of DNA barcodes in plant taxonomy. This approach offers a precise and dependable method for identifying medicinal *Rehmannia* plants and other herbal medicines.

Material and Methods

Experimental materials: In this study, fresh leaves of *Rehmannia* species were utilized as experimental samples, collected from various cities and counties across China. Additionally, certain ITS2 sequences of the *Rehmannia* and *Triaenophora* genera were extracted from the GenBank database (https://www.ncbi.nlm.nih.gov/genbank/), as outlined in (Table 2).

Sequence splicing and proofreading: The sequencing results indicated that the sequencing peak maps for the majority of target sequences displayed clear, stable, and tidy baselines. However, some low-quality regions with nested peaks were observed, particularly at the two ends of the target sequences. To eliminate low-quality fragments and primer regions, sequence splicing and refinement from the sequencing atlas were executed using CodonCode Aligner 5.1.1 and DNAstar 7.0 (Duan *et al*., 2019). Following this, manual proofreading of low-quality peak maps was conducted by incorporating sequence information from the GenBank database and assessing the Q value of the base.

The ITS2 sequences were aligned in GenBank using BLAST and compared with Clustal X 2.1. Subsequently, the alignment length, conserved sites, variable sites, and parsimony-informative sites among ITS2 sequences were further analyzed using MEGA 5.0.

Analysis of secondary structure and motif: In our investigation, we employed the ITS2 database (http://its2.bioapps.biozentrum.uni-wuerzburg.de/) to predict the secondary structure of ITS2 sequences within the *Rehmannia* and *Triaenophora* genera (Table S1). The specified parameters for this analysis were set as follows: E-value < 1e-16, incorporating force homology modeling as outlined by Merget *et al*., (2012). Subsequently, we conducted an analysis to discern the differences in the secondary structure of ITS2.

Additionally, we conducted an analysis of motifs within ITS2 sequences from the *Rehmannia* and *Triaenophora* genera using the ITS2 database, considering a maximum E-value (E<0.01). For the prediction of the consensus secondary structure of ITS2, we applied the ITS2 database pipeline, as detailed by Merget *et al*., (2012) and Koetschan *et al*., (2012).

Results

The characteristics of ITS2 sequence: We systematically analyzed the amplified ITS2 sequences, combining them with pertinent data retrieved from the GenBank database to ensure a comprehensive exploration of sequences. Subsequent detailed analysis highlighted that these variant sites predominantly involve substitutions between A-T, A-C, A-G, C-T, C-G, and G-T, with a particular emphasis on C-T and A-G variations (Table 1). This suggests a significant presence of base substitutions, particularly between purine and purine, as well as pyrimidine and pyrimidine, within the ITS2 sequences of *Rehmannia*.

Table 1. Distribution of variant sites in ITS2 sequences of *Rehmannia.*

Variant type	Variant loci
A-T	17, 43, 195, 224
C-T	19, 23, 33, 36, 65, 74, 77, 151, 155, 163, 164, 212, 225
C-G	51
A-G	73, 75, 157, 160, 165, 172, 184, 196, 202, 218
G-T	62, 76, 85, 179, 204
A-C	121, 140, 217
1 bp insertion/ deletion	21

Phylogenetic tree of ITS2 sequence: In this study, we reconstructed an NJ phylogenetic tree utilizing the ITS2 sequences of *Rehmannia* and its associated genus *Triaenophora*, as provided by Duan (2019) (Fig. 1). It was observed that all *Rehmannia* samples exhibited cohesive clustering, distinctly separate from *Triaenophora*. *Rehmannia* was partitioned into two major branches: Branch I and Branch II. Further subdivision of Branch I revealed two distinct sub-branches. Sub-branch I encompassed all samples of *R. glutinosa* and *R. solanifolia*, while Sub-branch II exhibited the clustering of *R. henryi* or *R. chingii*, each demonstrating evident monophyletic characteristics.

In Branch II, the samples of *R. piasezkii* and *R. elata* clustered together with a robust support rate exceeding 90%, distinctly separate from other *R. glutinosa* species. This observation underscores the clear differentiation among species within *Rehmannia* and *Triaenophora* based on ITS2 sequences. However, certain species in *Rehmannia*, such as *R. glutinosa* and *R. solanifolia*, and *R. piasezkii* and *R. elata*, were indistinguishable, suggesting a close genetic relationship between these pairs.

Table 2. The helix distribution in ITS2 sequence.

Species	GI	AC	Location of helix			
			Helix I	Helix II	Helix III	Helix IV
R. elata	67633929	DQ069315	0, 60	61, 88	96, 189	202, 220
R. solanifolia	67633928	DQ069314	3, 62	64, 91	99, 192	205, 223
R. glutinosa	161378249	EU266023	3, 61	63, 90	98, 191	204, 222
R. glutinosa	225348516	FJ770218	3, 62	64, 91	99, 192	205, 223
R. glutinosa	225348520	FJ770222	3, 62	64, 91	99, 192	205, 223
R. glutinosa	225348519	FJ770221	3, 62	64, 91	99, 192	205, 223
R. glutinosa	67633926	DQ069312	3, 62	64, 91	99, 192	205, 223
R. henryi	146262413	EF363671	3, 61	63, 90	98, 191	204, 222
R. henryi	82502192	DQ272447	3, 61	63, 90	98, 191	204, 222
R. chingii	67633927	DQ069313	3, 61	63, 90	98, 191	204, 222
R. piasezkii	146262412	EF363670	3, 61	63, 90	98, 191	204, 222
R. piasezkii	67633930	DQ069316	3, 61	63, 90	98, 191	204, 222
T. rupestris	154722033	EF522182	3, 58	61, 92	98, 194	207, 225
T. shennongjiaensis	-	FJ172741	8, 55	61, 92	98, 194	207, 225
T. rupestris	-	EF363675	8, 55	61, 92	98, 194	207, 225

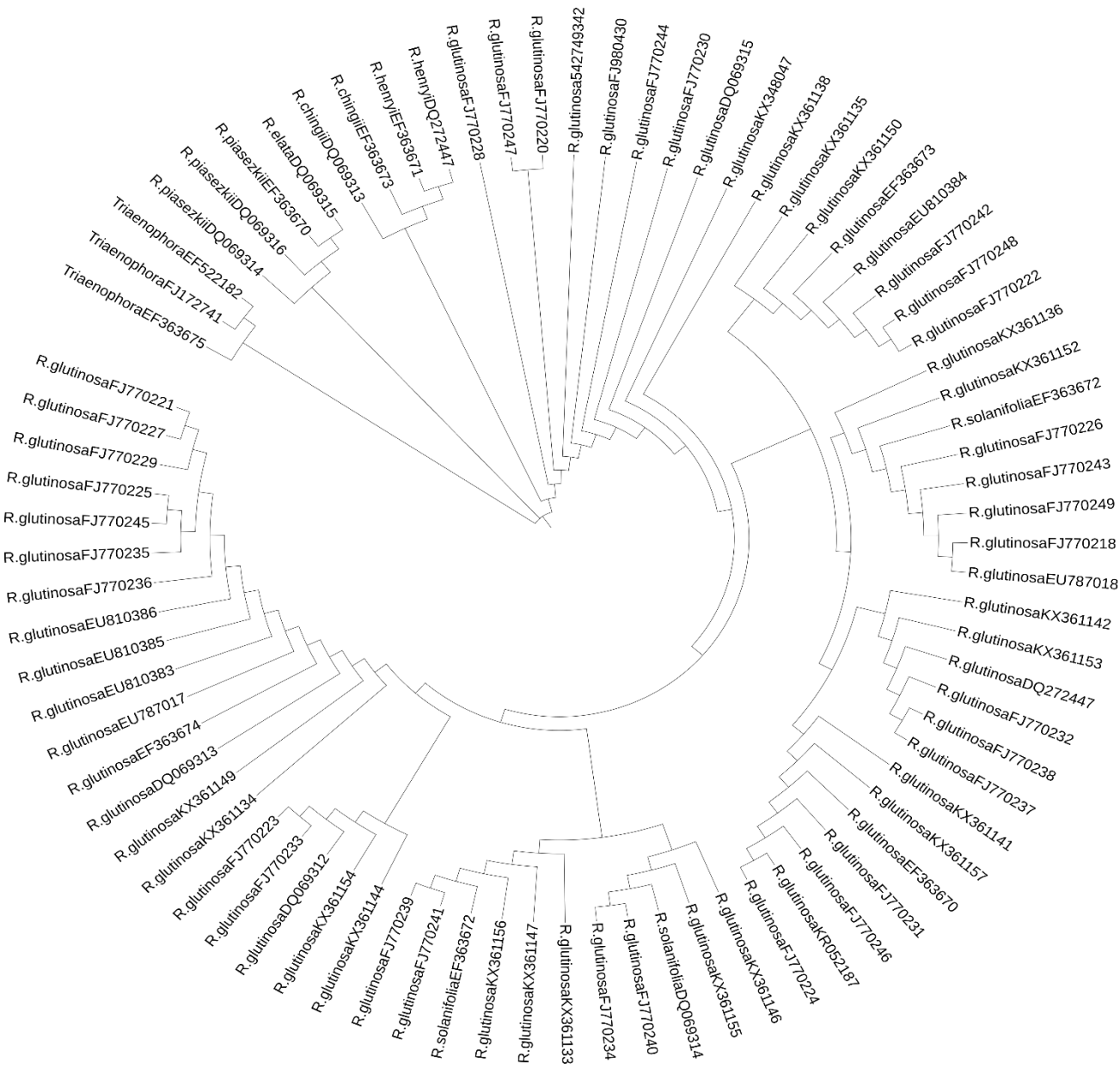

Fig. 1. Phylogenetic tree of *Rehmannia* based on ITS2 sequence.
The bootstrap scores (1000 replicates) are shown (≥50%) for each branch.

Table S1. Samples and ITS2 GenBank accession number of *Rehmannia* and *Triaenophora*.

No.	Species	Herb name	Genus	Source	GenBank No.
1.	*R. glutinosa*	Shangzuo1	*Rehmannia*	WIAS	KX361133
2.	*R. glutinosa*	Shangxibeixiang	*Rehmannia*	WIAS	KX361134
3.	*R. glutinosa*	Jinxiandiaoyu	*Rehmannia*	WIAS	KX361135
4.	*R. glutinosa*	Mixianyesheng	*Rehmannia*	WIAS	KX361136
5.	*R. glutinosa*	Hongshuwang	*Rehmannia*	WIAS	KX361137
6.	*R. glutinosa*	Guoxianshouji	*Rehmannia*	WIAS	KX361138
7.	*R. glutinosa*	Huanghouza	*Rehmannia*	WIAS	KX361139
8.	*R. glutinosa*	Yesheng	*Rehmannia*	WIAS	KX361140
9.	*R. glutinosa*	Xiuwufangzhuang	*Rehmannia*	WIAS	KX361141
10.	*R. glutinosa*	Wenhuai	*Rehmannia*	WIAS	KX361142
11.	*R. glutinosa*	Jinzhuangyuan	*Rehmannia*	WIAS	KX361143
12.	*R. glutinosa*	Fanshandihuang	*Rehmannia*	WIAS	KX361144
13.	*R. glutinosa*	Shangzuo2	*Rehmannia*	WIAS	KX361145
14.	*R. glutinosa*	Zhangsi961	*Rehmannia*	WIAS	KX361146
15.	*R. glutinosa*	Zhangsi901	*Rehmannia*	WIAS	KX361147
16.	*R. glutinosa*	Jinjiu	*Rehmannia*	WIAS	KX361148
17.	*R. glutinosa*	Dihuang	*Rehmannia*	JCJSC	KX361149
18.	*R. glutinosa*	Dihuang	*Rehmannia*	MWCJSC	KX361150
19.	*R. glutinosa*	Dihuang	*Rehmannia*	MTTCJSC	KX361151
20.	*R. glutinosa*	Dihuang	*Rehmannia*	HNUXHC	KX361152
21.	*R. glutinosa*	Dihuang	*Rehmannia*	LCHC	KX348047
22.	*R. glutinosa*	Lieyedihuang	*Rehmannia*	ECNUSC	KX361157
23.	*R. glutinosa*	Dihuang	*Rehmannia*	SDLHC	KX361153
24.	*R. glutinosa*	Dihuang	*Rehmannia*	WHC	KX361154
25.	*R. glutinosa*	Dihuang	*Rehmannia*	HCHC	KX361155
26.	*R. glutinosa*	Dihuang	*Rehmannia*	SDXHC	KX361156
27.	*R. chingii*	-	*Rehmannia*	Genbank	DQ069313
28.	*R. chingii*	-	*Rehmannia*	Genbank	EF363673
29.	*R. solanifolia*	-	*Rehmannia*	Genbank	DQ069314
30.	*R. solanifolia*	-	*Rehmannia*	Genbank	EF363672
31.	*R. elata*	-	*Rehmannia*	Genbank	DQ069315
32.	*R. piasezkii*	-	*Rehmannia*	Genbank	DQ069316
33.	*R. piasezkii*	-	*Rehmannia*	Genbank	EF363670
34.	*R. henryi*	-	*Rehmannia*	Genbank	DQ272447
35.	*R. henryi*	-	*Rehmannia*	Genbank	EF363671
36.	*R. glutinosa*	-	*Rehmannia*	Genbank	DQ069312
37.	*R. glutinosa*	-	*Rehmannia*	Genbank	EF363674
38.	*R. glutinosa*	-	*Rehmannia*	Genbank	EU266023
39.	*R. glutinosa*	-	*Rehmannia*	Genbank	EU266024
40.	*R. glutinosa*	-	*Rehmannia*	Genbank	EU266025
41.	*R. glutinosa*	85-5	*Rehmannia*	Genbank	EU787017
42.	*R. glutinosa*	DH9302	*Rehmannia*	Genbank	EU787018
43.	*R. glutinosa*	85-5	*Rehmannia*	Genbank	EU810383
44.	*R. glutinosa*	85-5	*Rehmannia*	Genbank	EU810384
45.	*R. glutinosa*	DH9302	*Rehmannia*	Genbank	EU810385

Table S1. (Cont'd.).

No.	Species	Herb name	Genus	Source	GenBank No.
46.	*R. glutinosa*	DH9302	*Rehmannia*	Genbank	EU810386
47.	*R. glutinosa*	Dahongpao	*Rehmannia*	Genbank	FJ770218
48.	*R. glutinosa*	Huixian	*Rehmannia*	Genbank	FJ770220
49.	*R. glutinosa*	Fengqiu	*Rehmannia*	Genbank	FJ770221
50.	*R. glutinosa*	Fengqiu	*Rehmannia*	Genbank	FJ770222
51.	*R. glutinosa*	Guolimao	*Rehmannia*	Genbank	FJ770223
52.	*R. glutinosa*	Huanghouza	*Rehmannia*	Genbank	FJ770224
53.	*R. glutinosa*	Huixian	*Rehmannia*	Genbank	FJ770225
54.	*R. glutinosa*	Jinsanyuan	*Rehmannia*	Genbank	FJ770226
55.	*R. glutinosa*	Jiyuanyesheng x 3kuai	*Rehmannia*	Genbank	FJ770227
56.	*R. glutinosa*	Jiyuanyesheng x 3kuai	*Rehmannia*	Genbank	FJ770228
57.	*R. glutinosa*	Jiyuanyesheng x No.2 Beijing	*Rehmannia*	Genbank	FJ770229
58.	*R. glutinosa*	Kangyu831	*Rehmannia*	Genbank	FJ770230
59.	*R. glutinosa*	Maye	*Rehmannia*	Genbank	FJ770231
60.	*R. glutinosa*	Qingtianhe	*Rehmannia*	Genbank	FJ770232
61.	*R. glutinosa*	Qingtianhe	*Rehmannia*	Genbank	FJ770233
62.	*R. glutinosa*	Huixian	*Rehmannia*	Genbank	FJ770234
63.	*R. glutinosa*	Sankuai	*Rehmannia*	Genbank	FJ770235
64.	*R. glutinosa*	Qingtianhe	*Rehmannia*	Genbank	FJ770236
65.	*R. glutinosa*	Shennongshan	*Rehmannia*	Genbank	FJ770237
66.	*R. glutinosa*	Shennongshan	*Rehmannia*	Genbank	FJ770238
67.	*R. glutinosa*	Shennongshan	*Rehmannia*	Genbank	FJ770239
68.	*R. glutinosa*	Shennongshan	*Rehmannia*	Genbank	FJ770240
69.	*R. glutinosa*	Shennongshan	*Rehmannia*	Genbank	FJ770241
70.	*R. glutinosa*	Shennongshan	*Rehmannia*	Genbank	FJ770242
71.	*R. glutinosa*	Shizitou	*Rehmannia*	Genbank	FJ770243
72.	*R. glutinosa*	Beijing No.3	*Rehmannia*	Genbank	FJ770244
73.	*R. glutinosa*	Huixian	*Rehmannia*	Genbank	FJ770245
74.	*R. glutinosa*	Xinzheng	*Rehmannia*	Genbank	FJ770246
75.	*R. glutinosa*	Dihuang85-5 x Maye F1	*Rehmannia*	Genbank	FJ770247
76.	*R. glutinosa*	Dihuang9302 x Jinzhuangyuan F2	*Rehmannia*	Genbank	FJ770248
77.	*R. glutinosa*	Zhangshi	*Rehmannia*	Genbank	FJ770249
78.	*R. glutinosa*	-	*Rehmannia*	Genbank	FJ980430
79.	*R. glutinosa*	-	*Rehmannia*	Genbank	KC463826
80.	*R. glutinosa*	-	*Rehmannia*	Genbank	KC463825
81.	*R. glutinosa*	-	*Rehmannia*	Genbank	KC463827
82.	*R. glutinosa*	-	*Rehmannia*	Genbank	KC463828
83.	*R. glutinosa*	-	*Rehmannia*	Genbank	KC463829
84.	*R. glutinosa*	-	*Rehmannia*	Genbank	KC463830
85.	*T. rupestris*	-	*Triaenophora*	Genbank	EF522182
86.	*T. shennongjiaensis*	-	*Triaenophora*	Genbank	FJ172741
87.	*T. rupestris*	-	*Triaenophora*	Genbank	EF363675

WIAS: Wenxian institute of agricultural sciences, Henan, China; JCJCSC: Junbu, Changqing district, Jinan, Shandong, China; MWCJSC: Mount Wenchang, Changqing district, Jinan, Shandong, China; MTTCJSC: Mount Tai, Taian County, Jinan, Shandong, China; ECNUSC: East China Normal University, Shanghai, China; HNUXHC: Henan Normal University, Xinxiang, Henan, China; LCHC: Lingbao County, Henan, China; SDLHC: Suburban district, Luohe, Henan, China; WHC: Weihui, Henan, China; HCHC: Hui County, Henan, China; SDXHC: Suburban district, Xinxiang, Henan, China

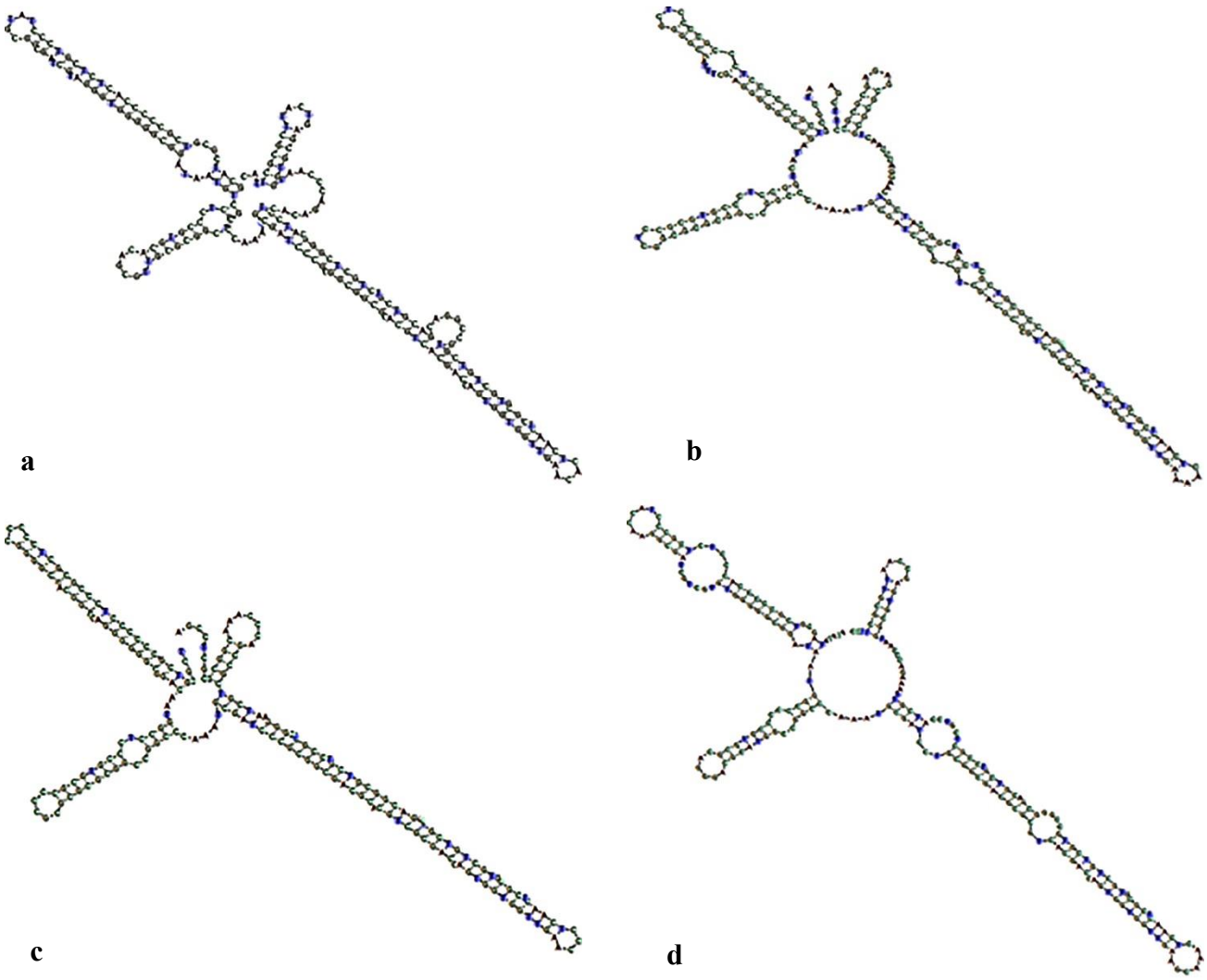

Fig. 2. The secondary structure model of ITS2 sequences in *Rehmannia* and *Triaenophora*
(a) The secondary structure and ribotype of ITS2 according to DQ069315 (*R. elata*), (b) The secondary structure and ribotype of ITS2 according to AF375147 (*F. lanceolata*), (c) The secondary structure and ribotype of ITS2 according to KJ563196 (*P. fortunei*), (d) The secondary structure and ribotype of ITS2 according to EF522182 (*T. rupestris*).

Homology model of ITS2 structure: As depicted in Fig. 2, the ITS2 secondary structure in *Rehmannia* and *Triaenophora* generally comprised of a central loop and four helices, namely helix I, helix II, helix III, and helix IV. Helix I and helix III exhibited longer lengths, while helix II and helix IV were comparatively shorter (Table 2). Distinct variations in the number and size of stems and loops were evident in each helix. While the ITS2 structure in *Triaenophora* bore similarity to that in *Rehmannia*, noteworthy differences existed between these two genera. In *Triaenophora*, helix I was shorter, and the number of loops was significantly reduced compared to *Rehmannia*. Additionally, helix III in *Triaenophora* displayed a lower number of loops in comparison to *Rehmannia* (Table 2, Fig. 2).

In our investigation, the observed polymorphisms in ITS2 sequences within *Rehmannia* delineated three distinct ribotypes (Fig. 2, a-c). Ribotype 1 encompassed of all *Rehmannia* species except for *R. glutinosa* No.2 Beijing (FJ770219) and No.1 Huixian (FJ770220) (Fig. 2, a). Ribotypes 2 and 3 were exclusive to FJ770219 and FJ770220, respectively (Fig. 2, b and c). Detailed similarities with the structure model DQ069315 (*R. elata*) are documented in (Table 3), revealing a high degree of similarity in each helix of ITS2 structures in *Rehmannia*. Notably, helix II and helix IV exhibited 100% similarity, with the exception of *R. glutinosa* EU266023, EU266025, FJ770221, and FJ770227. Most of helix 3 displayed a 97.368% similarity with the structure model, reaching 100% for DQ069313 (*R. chingii*), EF363670, or DQ069316 (*R. Piasezkii*).

Additionally, each helix of the ITS2 structure in *Triaenophora* exhibited high similarity with its corresponding structure model EF522182 (*T. rupestris*), surpassing 94%, and reaching 100% for helix II or helix IV (Table 4). Furthermore, the results of force homology modeling suggested that the transferred structure of ITS2 in *Triaenophora* closely resembled that of FJ770228 (*R. glutinosa*), DQ272447 (*R. henryi*), and AF375147 (*F. lanceolata*) (Table 4). Notably, this similarity was particularly evident in Helix I and Helix III, with values exceeding 85% when compared to *Rehmannia*. However, the least similarity was observed in Helix IV with *Rehmannia*, especially lower than in Helix IV with AF375147 (*F. lanceolata*), registering only at 33.333%.

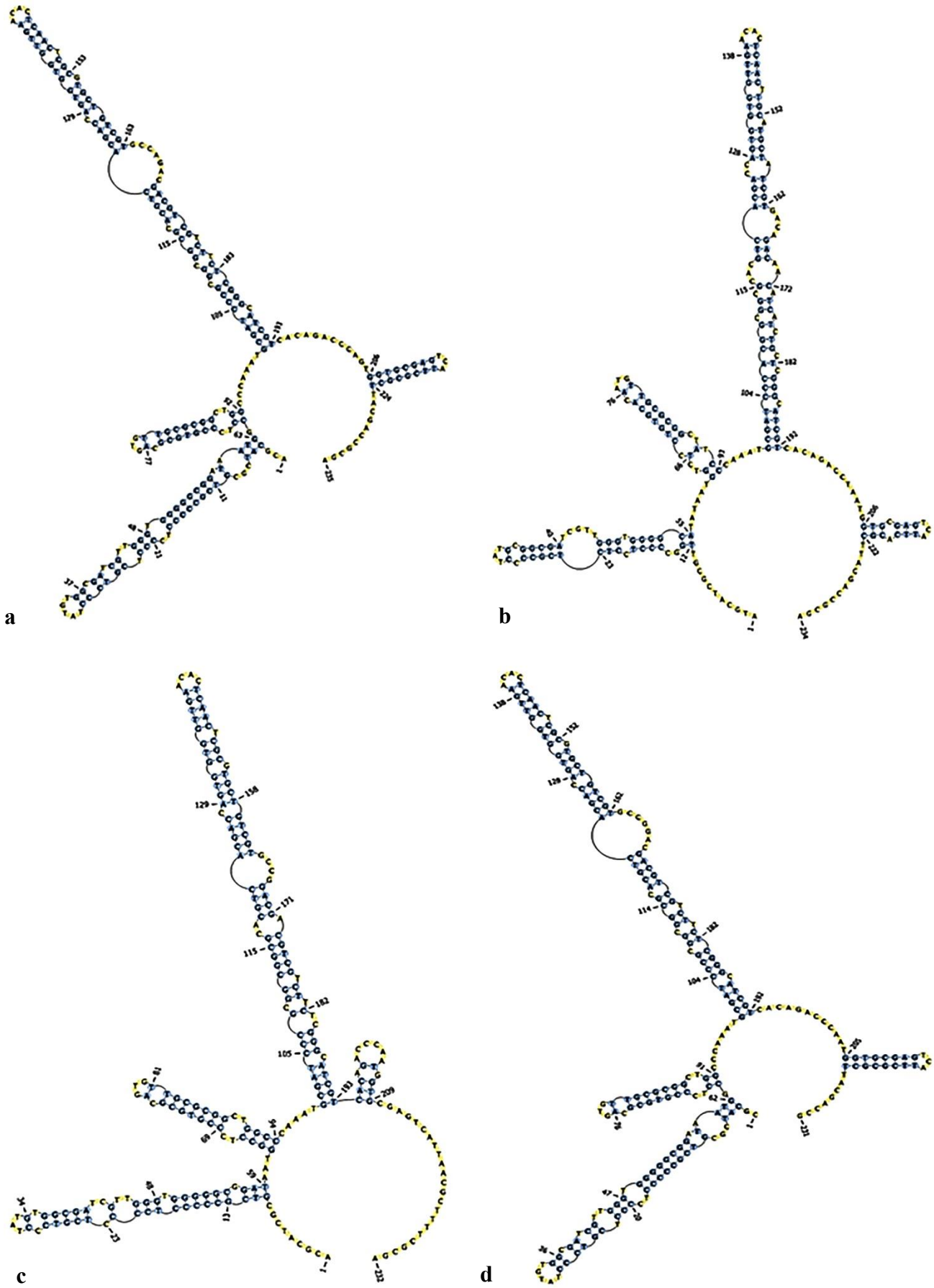

Fig. 3. Main types of ITS2 secondary structure in *R. glutinosa*
(a), (b), (c) and (d) represents the secondary structure of ITS2 sequence in *R. glutinosa*, such as FJ770218 (*R. glutinosa* Dahongpao), FJ770219 (*R. glutinosa* No.2 Beijing), FJ770220 (*R. glutinosa* No.1 Huixian), KC463825 (*R. glutinosa* voucher YC0129MT25), respectively.

Table 3. The transferred structure of ITS2 in *Rehmannia* from the model DQ069315.

Species	GI	AC	Helical transfer (%)				Score	Identity	Gap	Mismatches
			Helix I	Helix II	Helix III	Helix IV				
R. glutinosa	161378249	EU266023	78.261	100	86.842	85.714	740	199	12	24
R. glutinosa	161378250	EU266024	86.957	100	97.368	100	831	212	11	12
R. glutinosa	161378251	EU266025	86.957	100	89.474	100	805	207	11	17
R. glutinosa	193160873	EU787018	86.957	100	97.368	100	841	214	11	10
R. glutinosa	225348516	FJ770218	86.957	100	97.368	100	841	214	11	10
R. glutinosa	225348520	FJ770222	86.957	100	94.737	100	843	214	11	10
R. glutinosa	225348521	FJ770223	86.957	100	97. 638	100	849	215	11	9
R. glutinosa	225348522	FJ770224	82.609	100	94.737	100	838	214	11	10
R. glutinosa	225348523	FJ770225	86.957	100	94.737	100	830	212	11	12
R. glutinosa	193160847	EU787017	86.957	100	97. 638	100	854	216	11	8
R. glutinosa	193792562	EU810384	86.957	100	97. 638	100	854	216	11	8
R. glutinosa	225348524	FJ770226	86.957	100	97. 638	100	854	216	11	8
R. glutinosa	225348528	FJ770230	86.957	100	97. 638	100	854	216	11	8
R. glutinosa	225348529	FJ770231	86.957	100	97. 638	100	854	216	11	8
R. glutinosa	225348530	FJ770232	86.957	100	97. 638	100	854	216	11	8
R. glutinosa	225348531	FJ770233	86.957	100	97. 638	100	854	216	11	8
R. glutinosa	225348535	FJ770237	86.957	100	97. 638	100	854	216	11	8
R. glutinosa	225348538	FJ770240	86.957	100	97. 638	100	854	216	11	8
R. glutinosa	225348539	FJ770241	86.957	100	97. 638	100	854	216	11	8
R. glutinosa	225348540	FJ770242	86.957	100	97. 638	100	854	216	11	8
R. glutinosa	225348541	FJ770243	86.957	100	97. 638	100	854	216	11	8
R. glutinosa	225348542	FJ770244	86.957	100	97. 638	100	854	216	11	8
R. glutinosa	225348544	FJ770246	86.957	100	97. 638	100	854	216	11	8
R. glutinosa	225348546	FJ770248	86.957	100	97. 638	100	854	216	11	8
R. glutinosa	225348547	FJ770249	86.957	100	97. 638	100	854	216	11	8
R. glutinosa	238696040	FJ980430	86.957	100	97. 638	100	854	216	11	8
R. glutinosa	225348519	FJ770221	86.957	88.889	97. 638	100	840	214	11	10
R. glutinosa	225348525	FJ770227	86.957	88.889	97. 638	100	840	214	11	10
R. glutinosa	225348526	FJ770228	86.957	100	97. 638	100	844	214	11	10
R. glutinosa	193792561	EU810383	86.957	100	97. 638	100	849	215	11	9
R. glutinosa	193792563	EU810385	86.957	100	97. 638	100	849	215	11	9
R. glutinosa	193792564	EU810386	86.957	100	97. 638	100	849	215	11	9
R. glutinosa	225348527	FJ770229	86.957	100	97. 638	100	849	215	11	9
R. glutinosa	225348533	FJ770235	86.957	100	97. 638	100	849	215	11	9
R. glutinosa	225348543	FJ770245	86.957	100	97. 638	100	849	215	11	9
R. glutinosa	225348532	FJ770234	86.957	100	97. 638	100	849	215	11	9
R. glutinosa	225348534	FJ770236	86.957	100	94.737	100	843	214	11	10
R. glutinosa	225348536	FJ770238	86.957	100	94.737	100	843	215	11	9
R. glutinosa	225348537	FJ770239	86.957	100	97. 638	100	849	215	11	9
R. glutinosa	225348545	FJ770247	86.957	100	97. 638	100	849	215	11	9
R. glutinosa	542749365	KC463826	86.957	100	97. 638	100	854	216	7	8
R. glutinosa	542749342	KC463825	86.957	100	97. 638	100	854	216	7	8
R. glutinosa	542749400	KC463827	86.957	100	97. 638	100	854	216	7	8
R. glutinosa	542749432	KC463828	86.957	100	97. 638	100	854	216	7	8
R. glutinosa	542749457	KC463829	86.957	100	97. 638	100	854	216	7	8
R. glutinosa	542749482	KC463830	86.957	100	97. 638	100	854	216	7	8
R. glutinosa	67633926	DQ069312	86.957	100	97. 638	100	854	216	3	8
R. solanifolia	67633928	DQ069314	86.957	100	97.368	100	854	216	9	8
R. henryi	146262413	EF363671	91.304	100	100	85.714	842	211	10	13
R. henryi	82502192	DQ272447	91.304	100	100	85.714	842	211	10	13
R. chingii	67633927	DQ069313	91.304	100	100	100	879	216	2	8
R. piasezkii	146262412	EF363670	95.652	100	100	100	921	223	8	1
R. piasezkii	67633930	DQ069316	95.652	100	100	100	921	223	8	1

Table 4. Comparison of ITS2 structure in *Triaenophora* and their homology structures.

Species	GI	AC	EF522182 (*T. rupestris*)		FJ172741 (*T. shennongjiaensis*)		EF363675 (*T. rupestris*)	
			Helical transfer (%)	E-Value	Helical transfer (%)	E-Value	Helical transfer (%)	E-Value
T.rupestris	154722033	EF522182	Helix I 100 Helix II 100 Helix III 100 Helix IV 100	1.744	94.118 100 97.143 100	4.886	94.118 100 97.143 100	3.777
R. glutinosa	225348526	FJ770228	Helix I 85.714 Helix II 80 Helix III 86.486 Helix IV 62.5	2.457	86.364 80 89.474 71.429	4.119	86.364 80 89.474 71.429	4.111
R. henryi	82502192	DQ272447	Helix I 86.364 Helix II 80 Helix III 86.842 Helix IV 71.429	8.900	85.714 80 89.189 62.5	1.135	85.714 80 89.189 62.5	1.135
F. lanceolata	20339368	AF375147	Helix I 81.25 Helix II 83.333 Helix III 86.486 Helix IV 33.333	5.433	81.25 83.333 83.784 33.333	5.433	81.25 83.333 83.784 33.333	5.433

Secondary structure of ITS2 sequence: As depicted in Fig. S1, significant interspecific differences in the ITS2 secondary structure were observed among the six *Rehmannia* species. These differences manifested in diverse angles between helices, varying helix lengths, and discrepancies in the number and shape of stems or loops within each helix. For instance, the structure of DQ069313 (*R. chingii*) displayed 6 loops in helix I, 3 loops in helix II, 9 loops in helix III, and only 1 loop in helix IV (Fig. S1, a). Building upon DQ069313, the structure of DQ069315 (*R. elata*) featured 5 loops in helix I and 2 loops in helix II, with differing angles between helices (Fig. S1, c). While the angles between helices differed in DQ069316 (*R. piasezkii*) and DQ272447 (*R. henryi*), the number of loops remains consistent across all four helices (Fig. S1, d-f). The structure of DQ069314 (*R. solanifolia*) comprised of 7 loops in helix I and 10 loops in helix III. Notably, the number of loops aligned between DQ069312 (*R. glutinosa*) and DQ069314 (*R. solanifolia*), although the angles differed in their corresponding helices (Fig. S1, b and f).

Further analysis revealed minimal intra-species variation in the ITS2 secondary structure within the *Rehmannia* genus. For instance, the secondary structures of *R. solanifolia* (DQ069314) and *R. piasezkii* (DQ069316) (Fig. 4, b and Fig. 4, d) exhibited striking similarity, displaying nearly identical overall structures, helix count, angles, sizes, and lengths. Similarly, the secondary structures of *R. chingii* (DQ069313) and *R. glutinosa* (DQ069312) (Fig. S1, a and Fig. S1, f) were nearly indistinguishable in terms of overall structure, helix count, angles, sizes, and lengths. Nevertheless, notable differences were observed in the ITS2 structure of *R. glutinosa*, particularly between DQ069312 and FJ770220 (Fig. S1, f and Fig. S1, c). The ITS2 structure of *R. glutinosa* was further classified into four main types (Fig. 3), with the primary distinction among most *R. glutinosa* species being the number of helices in the central loop. However, the structures of most *R. glutinosa* species closely resembled that of FJ770218 (Fig. 3, a), including examples such as FJ770221, FJ770222, FJ770224, FJ770225, FJ770227, FJ770236, FJ220238, and others. Consequently, significant differences in the ITS2 structures were identified among the 6 *Rehmannia* species, yet structural similarities were observed among closely related species.

Furthermore, distinctions in the ITS2 structures of *Triaenophora* were evident, encompassing variations in helix length, diverse angles between helices, and discrepancies in the number and shape of stems or loops within helices (Fig. S1, g-i). In the case of EF522182 (*T. rupestris*), helices I, II, and IV exhibited a sequential loop count of 3, 2, and 1, respectively, while helix III presented 3 large loops and 5 small loops (Fig. S1, d). A comparative analysis presented in Fig. S1 (g-i) revealed the identical ITS2 structure of FJ172741 (*T. shennongjiaensis*) and EF363675 (*T. rupestris*). In contrast to EF522182 (*T. rupestris*), helix I in FJ172741 had 2 loops, the positions of 5 small loops in helix III were dispersed, and variations in angles between helices were observed.

The motifs of ITS2 sequence: In Table S2, the ITS2 sequences in *Rehmannia* exhibited consistent motifs, characterized by U-U mismatch (II, left), U-U mismatch (II, right), and UGGU (III, 5' side), predominantly situated at positions 57-73 bp, 85-100 bp, and 124-138 bp, respectively (see Fig. 4). Notably, the ITS2 sequences of *R. glutinosa* FJ770219, FJ770221, and FJ770227 displayed a simplified composition, featuring only two components: U-U mismatch (II, left) and UGGU (Fig. 4, g-i). Furthermore, the U-U mismatch (II, left), U-U mismatch (II, right), and UGGU motifs in *Rehmannia* consistently comprised 15 base pairs, with three distinct sequences observed for U-U mismatch (II, left): TAATGGCCTCCCGTG, TAATGTCCTCCTGTG, or TAATGGCCCCCCGTG. The sequences for U-U mismatch (II, right) and UGGU are CGGCTGGCCCAAATG and GACCAGTGGTGGTTG, respectively, in *Rehmannia* (refer to Table S2). This observed uniformity underscores the relative conservation of the ITS2 motif, with identical base sequences prevalent across the majority of motifs in *Rehmannia*.

Moreover, within *Triaenophora*, the ITS2 sequences exclusively feature U-U mismatch (II, left) and UGGU motifs, positioned at 58-72 bp and 124-138 bp, respectively (refer to Table S2). The specific sequences for U-U mismatch and UGGU are TAATGGCCCCCCGTG and GACCAGTGGTGGTTG, respectively (see Table S2).

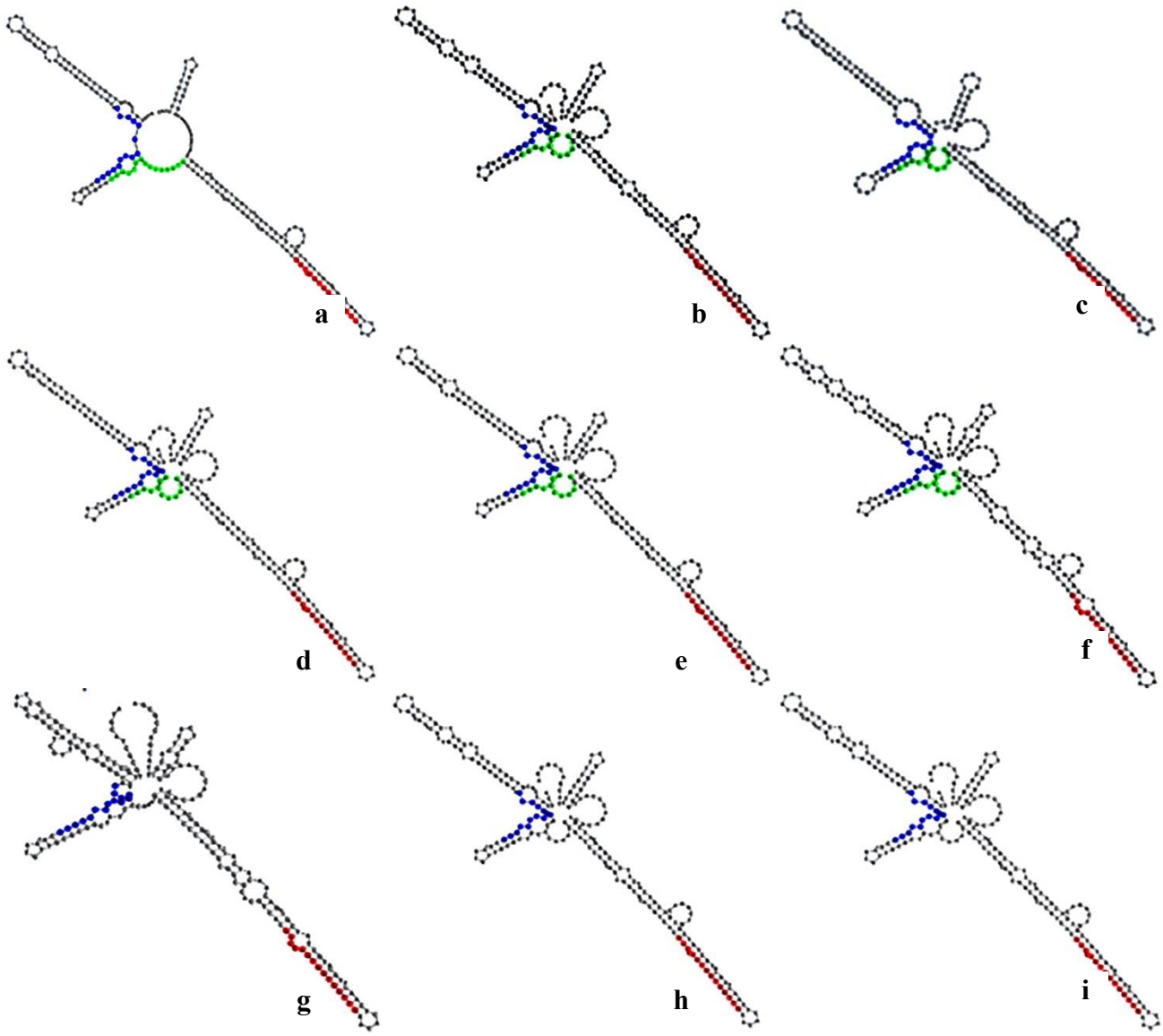

Fig. 4. The motifs of ITS2 sequences in *Rehmannia*
(a), (b), (c), (d), (e), (f), (g), (h) and (i) respectively represents the motifs of ITS2 sequence in *Rehmannia*, such as *R. chingii* (DQ069313), *R. solanifolia* (DQ069314), *R. elata* (DQ069315), *R. piasezkii* (DQ069316), *R. henryi* (DQ272447), *R. glutinosa* (EU266023), *R. glutinosa* (FJ770219), *R. glutinosa* (FJ770221) and *R. glutinosa* (FJ770227). The motif of U-U mismatch (II, left), U-U mismatch (II, right) and UGGU (III, 5'side) in ITS2 sequence is shown blue, green and red, respectively

Discussions

Ribosomal DNA (rDNA) is widely acknowledged as the shared genetic material in both male and female lineages, holding significant importance in the realms of species classification and evolution (Shinwari, 2002). The ITS2 sequence, situated within the transcribed spacer region of 5.8-26S ribosomal DNA, is characterized by a plethora of variant points and informative sites (Coleman, 2007; Miao *et al*., 2008). These features endow ITS2 with a robust capacity to discriminate among plants, making it a valuable tool for applications in phylogeny and species identification (Luo *et al*., 2010; Chen *et al*., 2010; Gao *et al*., 2011; Shinwari *et al*., 2014). In recent years, the ITS2 sequence has found widespread application in the classification and identification of plant species, particularly in the context of Chinese herbal medicines (Chen *et al*., 2010; Liu *et al*., 2012; Ren *et al*., 2017).

The roots of *R. glutinosa* and its related species possess medicinal properties, with *R. glutinosa* serving as the primary plant source for the renowned traditional Chinese herbal medicine known as Di Huang (Duan *et al*., 2019). Di Huang has gained prominence not only within China but has also been introduced to other nations, including Japan and South Korea. Currently, the market presents challenges in discerning the diverse sources of Di Huang medicine, necessitating correct identification processes (Xia & Li, 2009). In our study, the ITS2 sequence in *Rehmannia* spans approximately 224-235bp, exhibiting a GC content ranging from 64.22% to 66.67%. The mutation rate is recorded at 16.0%, revealing numerous base substitutions between pyrimidine-pyrimidine and purine-purine within the ITS2 sequence of *Rehmannia*. Subsequent analysis revealed that the ITS2 sequence demonstrates greater interspecific diversity and lower intraspecific divergence within *Rehmannia*. Nevertheless, according to the NJ phylogenetic

tree of ITS2 sequences, it appears that *R. glutinosa* and *R. solanifolia*, as well as *R. elata* and *R. piasezkii*, may be considered relatively close relatives (Duan *et al*., 2019). Chen *et al*., (2010) reported a remarkable identification efficiency of 92.7% at the species level for 4800 medicinal plants across 753 genera using the ITS2 sequence. Furthermore, Ren *et al*., (2017) demonstrated the accurate identification of medicinal plants belonging to the *Artemisia odorats* and its related genera through the application of the ITS2 sequence. Additionally, ITS2 sequence was successfully employed for the efficient identification of *Hedyotis diffusa* and its counterfeits, highlighting the broad applicability of this approach (Yan *et al*., 2015). Consequently, the use of the ITS2 sequence emerges as an effective means for plant identification, ensuring the safety and authenticity of clinical drugs.

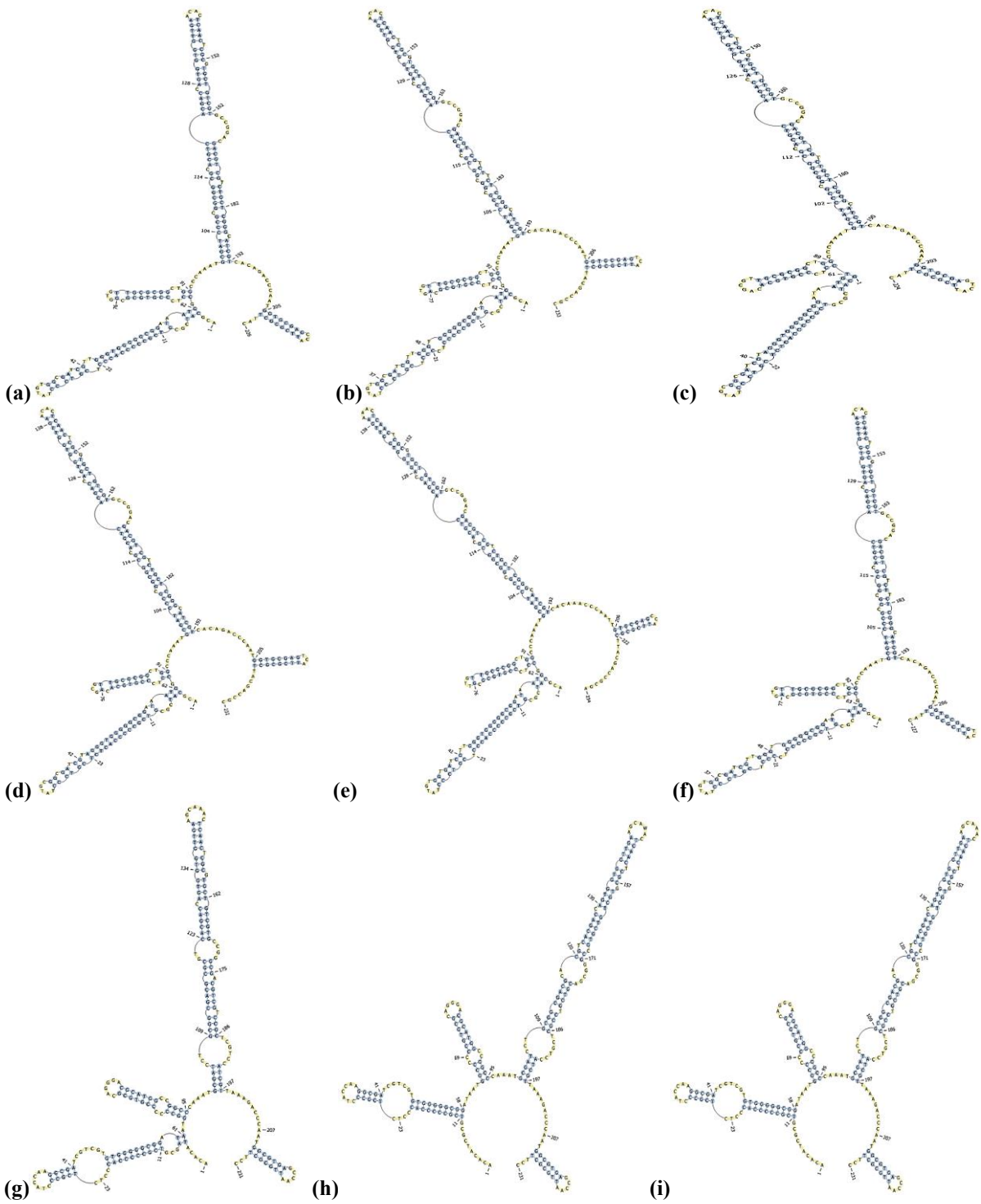

Fig. S1. The secondary structure of ITS2 sequences in *Rehmannia* and *Triaenophora*
(a), (b), (c), (d), (e) and (f) represents the secondary structure of ITS2 in six species of *Rehmannia*, such as *R. chingii* (DQ069313), *R. solanifolia* (DQ069314), *R. elata* (DQ069315)*, R. piasezkii* (DQ069316), *R. henry* (DQ272447), *R. glutinosa* (DQ069312), respectively. (g), (h) and (i) represents the secondary structure of ITS2 in *Triaenophora*, such as *T. rupestris* (EF522182), *T. shennongjiaensis* (FJ172741), *T. rupestris* (EF363675), respectively.

Beyond its utility in genetic analysis, the ITS2 sequence's secondary structure offers valuable insights into key evolutionary patterns, enhancing the phylogenetic resolution (Coleman & van Oppen, 2008). Wiemers *et al*., (2009) demonstrated that the secondary structure of ITS2 significantly improves phylogeny estimation, particularly in the butterfly family Lycaenidae. This structural information can be leveraged for feature-based phylogenetic analysis, extending beyond the traditional sequence-based ITS2 phylogeny, as observed in studies by Zhu *et al*., (2018) and Zhang *et al*., (2020). Within this investigation, the secondary structure analysis of ITS2 in both *Rehmannia* and its relative genus *Triaenophora* reveals a shared structural pattern comprising a central loop and four helices. Specifically, helix I and helix III exhibit longer lengths, while helix II and helix IV are comparatively shorter. Moreover, variations in the number and size of stems and loops are evident in each helix. Interestingly, when comparing the secondary structure of ITS2 in *Triaenophora* to that of *Rehmannia*, notable distinctions emerge, including a shorter helix I and a reduction in the number of loops in helix I and helix III in *Triaenophoras*. Coleman *et al*., (2007) have noted that ITS2 commonly exhibits four helices, with variable lengths and shapes across most eukaryotes. Additionally, in the ITS2 sequences of *Rehmannia* and *Triaenophora*, two motifs have been identified: the U-U mismatch (II, left) and UGGU. Notably, the sequences of UGGU are identical between the two genera, whereas the U-U mismatch has three distinct base sequences in *Rehmannia*. Interestingly, U-U mismatch (II, right) is also present in *Rehmannia*, except for several varieties of *R. glutinosa*. This observation underscores the relatively conserved nature of the motifs in ITS2, aligning with the corresponding ITS2 secondary structure (Van Nues *et al*., 1995; Mai & Coleman, 1997).

Currently, the application of ITS2 secondary structure for species classification and identification has gained traction (Adebowale *et al*., 2016; Samanta *et al*., 2018; Tasneem *et al*., 2019). Within our study, a pronounced interspecific difference is observed in the ITS2 secondary structure among the six *Rehmannia* species. This distinction is evident in various aspects, including the diverse angles between helices, distinct helix lengths, and variations in the number and shape of stems or loops within each helix. These findings align with previous research emphasizing the significance of such structural variations in species differentiation (Coleman, 2007; Wolf *et al*., 2005). The utility of ITS2 secondary structure enhances the discrimination of ITS2 sequences in various medicinal species, including *Hedyotis diffusa* (Yin *et al*., 2012), Mu Tong (Zhang *et al*., 2015), *Ligusticum* (Liu *et al*., 2019), among others. Notably, the ITS2 secondary structures of *R. glutinosa* display notable differences, categorized into four main types. Similarly, the original plants of certain traditional Chinese medicines can be effectively distinguished from relevant species and their adulterants based on ITS2, as demonstrated in *Gynostemma pentaphyllum* (Liu *et al*., 2012), *Eucommia ulmoides* (Peng *et al*., 2012), and *Fritillariae Cirrhosae bulbus* (Luo *et al*., 2012), among others. Thus, the ITS2 secondary structure significantly contributes to enhancing the universality of ITS2 in species identification and classification. Our study reconfirms the effectiveness of the ITS2 sequence in the identification of plant species, both in terms of primary sequence information and secondary structure. In various related research domains, such as herbal quality control, evolutionary studies, and biodiversity conservation, ITS2 demonstrates robust research potential and application value.

Conclusions

The ITS2 sequence, characterized by abundant variant points and informative sites, has found extensive application in the identification and classification of plant species. These findings suggest that the secondary structure plays a crucial role in enhancing the identification ability of ITS2, particularly in distinguishing related species and counterfeit varieties within *R. glutinosa*. Moreover, the species within *Rehmannia* exhibit clear differentiation from its relative genus *Triaenophora*, as evidenced by distinctive patterns in their ITS2 sequences. The motifs, lengths, and shapes of helices in the ITS2 secondary structure further contribute to the variability observed between *Rehmannia* and *Triaenophora*. Consequently, both the sequence and secondary structure of ITS2 demonstrate a noteworthy capability for species identification within *Rehmannia* and its relative genus *Triaenophora*. Notably, this ability effectively distinguish the original plants of the traditional Chinese herbal medicine Di Huang from relevant species and their potential adulterants based on ITS2.

Acknowledgements

This research is funded by the National Science Foundation of China (No. U1304304) and the Fund of Henan Province (No. 23IRTSTHN022 and No. 222301420097) in China. Additionally, the study received support from “The High Performance Computing Center of Henan Normal University.” Certain varieties of *R. glutinosa* were generously provided by Yongkang Liu and Cuihong Lu at the Agricultural Research Institute of Wenxian County, Henan, China.

References

Adebowale, A., J. Lamb, A. Nicholas and Y. Naidoo. 2016. ITS2 secondary structure for species circumscription: Case study in southern African *Strychnos* L. (Loganiaceae). *Genetica*, 144: 639-650.

Chase, M.W., R.S. Cowan and P.M. Hollingsworth. 2007. A proposal for a standardised protocol to barcode all land plants. *Taxon*, 56: 295-299.

Chen, P.L., X.Y. Wei, Q.T. Qi, W.J. Jia, M.W. Zhao, H.N. Wang, Y.Q. Zhou and H.Y. Duan. 2021. Study of terpenoid synthesis and prenyltransferase in roots of *Rehmannia glutinosa* based on iTRAQ quantitative proteomics. *Front. Plant Sci*., 12: 693758.

Chen, S.L., H. Yao, J.P. Han, C. Liu, J.Y. Song, L.C. Shi, Y.J. Zhu, X.Y. Ma, T. Gao, X.H. Pang, K. Luo, Y. Li, X.W. Li,

X.C. Jia, Y.L. Lin and C. Leon. 2010. Validation of the ITS2 region as a novel DNA barcode for identifying medicinal plant species. *PLoS One*, 5: e8613.

Coleman, A.W. 2007. Pan-eukaryote ITS2 homologies revealed by RNA secondary structure. *Nucl. Acids Res.*, 35: 3322-3329.

Coleman, A.W. and M.J. van Oppen. 2008. Secondary structure of the rRNA ITS2 region reveals key evolutionary patterns in acroporid corals. *J. Mol. Evol.*, 67: 389-396.

Duan, H.Y., W.S. Wang, Y.P. Zeng, M.M. Guo and Y.Q. Zhou. 2019. The screening and identification of DNA barcode sequences for *Rehmannia*. *Sci. Rep.*, 9: 17295.

Gao, T., Z. Sun, H. Yao, J. Song, Y. Zhu, X. Ma and S. Chen. 2011. Identification of Fabaceae plants using the DNA barcode *matK*. *Planta Med.*, 77: 92-94.

Hebert, P.D.N., S. Ratnasingham and J.R. Dewaard. 2003. Barcoding animal life: Cytochromecoxidase subunit 1 divergences among closely related species. *Proc. Biol. Sci.*, 270: 96-99.

Hollingsworth, P.M., L.L. Forrest, J.L. Spouge, M. Hajibabaei, S. Ratnasingham and others of CBOL Plant Working Group. 2009. A DNA barcode for land plants. *Proc. Natl. Acad. Sci. U.S.A.*, 106: 12794-12797.

Huang, Y., C.M. Jiang, Y.L. Hu, X.J. Zhao, C. Shi, Y. Yu, C. Liu, Y. Tao, H.R. Pan, Y.B. Feng, J.G. Liu, Y. Wu and D.Y. Wang. 2013. Immunoenhancement effect of *Rehmannia glutinosa* polysaccharide on lymphocyte proliferation and dendritic cell. *Carbohyd. Polym.*, 96: 516-521.

Koetschan, C., T. Hackl, T. Müller, M. Wolf, F. Förster and J. Schultz. 2012. ITS2 database IV: interactive taxon sampling for internal transcribed spacer 2 based phylogenies. *Mol. Phylogen. Evol.*, 63: 585-588.

Kress, W.J., K.J. Wurdack, E.A. Zimmer, L.A. Weigt and D.H. Janzen. 2005. Use of DNA barcodes to identify flowering plants. *Proc. Natl. Acad. Sci. U.S.A.*, 102: 8369-8374.

Liu, Y., Y.L. Tang, T. Wu, Y.S. Wu and D. Jiang. 2012. *Molecular identification of Gynostemma pentaphyllum and its counterfeits based on DNA barcoding (ITS2). China Foreign Med. Treat.*, 31: 105-106.

Liu, Z.W., Y.Z. Gao and J. Zhou. 2019. Molecular authentication of the medicinal species of *Ligusticum* (Ligustici Rhizoma et Radix, "Gao-ben") by integrating non-coding Internal Transcribed Spacer 2 (ITS2) and its secondary structure. *Front. Plant Sci.*, 10: 429.

Luo, K., P. Ma, H. Yao, J.Y. Song, K.L. Chen and Y.M. Liu. 2012. *Molecular identification of Fritillariae Cirrhosae Bulbus and its adulterants. Sci. Technol. Soc.*, 1: 1153-1158.

Luo, K., S.L. Chen, K.L. Chen, J.Y. Song, H. Yao, X.Y. Ma, Y.J. Zhu, X.H. Pang, H. Yu, X.W. Li and Z. Liu. 2010. Assessment of candidate plant DNA barcodes using the Rutaceae family. *Sci. China Life Sci.*, 53: 701-708.

Mai, J.C. and A.W. Coleman. 1997. The internal transcribed spacer 2 exhibits a common secondary structure in green algae and flowering plants. *J. Mol. Biol.*, 44: 258-271.

Merget, B., C. Koetschan, T. Hackl, F. Förster, T. Dandekar, T. Müller, J. Schultz and M. Wolf. 2012. The ITS2 Database. *J. Vis. Exp.*, 61: 3806.

Miao, M., A. Warren, W. Song, S. Wamg, H.M. Sjamg and Z.G. Chen. 2008. Analysis of the internal transcribed spacer 2 (ITS2) region of Scuticociliates and related taxa (Ciliophora, Oligohymenophorea) to infer their evolution and phylogeny. *Protist*, 159: 519-533.

Peng, Z., J.G. Zhu, J.X. Tan and L.B. Wang. 2012. *Identification of Eucommia ulmoides and its adulterants based on ITS2 sequences. Zhong Cao Yao*, 21: 3042-3047.

Pennisi, E. 2007. Taxonomy. Wanted: a barcode for plants. *Science*, 318: 190-191.

Ren, B.Q., X.G. Xiang and Z.D. Chen. 2010. Species identification of *Alnus* (Betulaceae) using nrDNA and cpDNA genetic markers. *Mol. Ecol. Resour.*, 10: 594-605.

Ren, Y.Y., N.P. Jiang, R.Y. Liu, L.K. Song, R. Tan and J. Gu. 2017. ITS2 sequence analysis and identification of medicinal Artemisia plants. *Zhongguo Zhong Yao Za Zhi*, 42: 1395-1400.

Samanta, B., J.M. Ehrman and I. Kaczmarska. 2018. A consensus secondary structure of ITS2 for the diatom Order Cymatosirales *(Mediophyceae, Bacillariophyta*) and reappraisal of the order based on DNA, morphology, and reproduction. *Mol. Phylogenet. Evol.*, 129: 117-129.

Shinwari, Z.K. 1995. Congruence between morphology and molecular phylogeneties in *Prosartes* (Liliaceae). *Pak. J. Bot.*, 27(2): 361-369.

Shinwari, Z.K. 1998. Molecular systematics of the genus *Uvularia* and related taxa based upon *rbcL* gene sequence data. *Pak. J. Bot.*, 30(2): 161-172.

Shinwari, Z.K. 2000. Chloroplast DNA variation in Polygonatae (Liliaceae). *Pak. J. Bot.*, 32(1): 7-14.

Shinwari, Z.K. 2002. Sequence divergence of *rbcL* gene and Phylogenetic relationships in *Liliales*. *Pak. J. Bot.*, 34(2): 191-204.

Shinwari, Z.K., H. Kato, R. Terauchi and S. Kawano. 1994a. Phylogenetic relationships among genera in *theliliaceae-Asparagoideae-Polygonatae* s.l. inferred from*rbcl* gene sequence data. *Plant Syst. Evol.*, 192(3-4): 263-277.

Shinwari, Z.K., K. Jamil and N.B. Zahra. 2014. Molecular systematics of selected genera of family Fabaceae. *Pak. J. Bot.*, 46(2): 591-598.

Shinwari, Z.K., R. Terauch and S. Kawano. 1994. Molecular Systematics of Liliaceae-Asparagoideae-Polygonatae. I. RFLP analysis of *cp*DNA in Several Asiatic *Disporum* Species. *Plant Species Biol.*, 9: 11-18.

State Pharmacopoeia Commission and Chinese Pharmacopoeia, 2015. *Beijing: China Medical Science and Technology Press.*

Tasneem, F., F.R. Shakoori, M. Ilyas, N. Shahzad, A. Potekhin and A.R. Shakoori. 2019. Genetic diversity of Paramecium species on the basis of multiple loci analysis and ITS secondary structure models. *J. Cell. Biochem.*, 121: 3837-3853.

Van Nues, R.W., J.M.J. Rientjes, S.A. Morré, E. Mollee, R.J. Planta, J. Venema and H.A. Raué. 1995. Evolutionarily conserved structural elements are critical for processing of internal transcribed spacer 2 from Saccharomyces cerevisiae precursor ribosomal RNA. *J. Mol. Biol.*, 250: 24-36.

Wang, J., X. Meng, R. Lu, C. Wu, Y.T. Luo, X. Yan, X.J Li., X.H. Kong and G.X. Nie. 2015. Effects of *Rehmannia glutinosa* on growth performance, immunological parameters and disease resistance to *Aeromonas hydrophila* in common carp (*Cyprinus carpio* L.). *Aquaculture*, 435: 293-300.

Wang, Y.B., Y.F. Liu, X.T. Lu, F.F. Yan, B. Wang, W.W. Bai and Y.X. Zhao. 2013. *Rehmannia glutinosa* extract activates endothelial progenitor cells in a rat model of myocardial infarction through a SDF-1 α/CXCR4 cascade. *PLoS One*, 8: e54303.

Wiemers, M., A. Keller and M. Wolf. 2009. *ITS2* secondary structure improves phylogeny estimation in a radiation of blue butterflies of the subgenus *Agrodiaetus* (Lepidoptera: Lycaenidae: *Polyommatus*). *BMC Evol. Biol.*, 9: 300.

Wolf, M., M. Achtziger, J. Schultz, T. Dandekar and T. Müller. 2005. Homology modeling revealed more than 20,000 rRNA internal transcribed spacer 2 (ITS2) secondary structures. *RNA*, 11: 1616-1623.

Xia, Z. and J.M. Li. 2009. Investigation on medicinal plant resources of *Rehamnania* and its relative genus *Triaenophora*. *J. Shangqiu Teachers College*, 25: 96-98.

Yan, S., W.C. Ren, X.L. Zheng, Y. Yang, B. Pan, Y.H. Shi, W. Sun and W. Ma. 2015. Survey of commercially available *Oldenlandia diffusa* products using DNA barcoding. *Mod. Chinese Med.*, 10: 1014-1019.

Yang, J.B., Y.P. Wang, M. Möller, L.M Gao and D. Wu. 2012. Applying plant DNA barcodes to identify species of *Parnassia* (*Parnassiaceae*). *Mol. Ecol. Resour.*, 12: 267-275.

Yin, X.M., K. Luo, M.Z. Liu and H.M. Luo. 2012. Molecular identification of *Cnidium monnieri* and its closely related species using ITS2 sequences. *Mod. Chinese Med.*, 3: 9-11.

Zhang, W., W. Tian, Z. Gao, G. Wang and H. Zhao. 2020. Phylogenetic utility of rRNA ITS2 sequence-structure under functional constraint. *Int. J. Mol. Sci.*, 21: 6395.

Zhang, W., Y. Yuan, S. Yang, J. Huang and L. Huang. 2015. ITS2 secondary structure improves discrimination between medicinal "Mu Tong" species when using DNA barcoding. *PLoS One*, 10: e0131185.

Zhu, S., Q. Li, S. Chen, Y. Wang, L. Zhou, C. Zeng and J. Dong. 2018. Phylogenetic analysis of *Uncaria* species based on internal transcribed spacer (ITS) region and ITS2 secondary structure. *Pharm. Biol.*, 56: 548-558.

Zuo, Y., Z. Chen, K. Kondo, T. Funamoto, J. Wen and S. Zhou. 2011. DNA barcoding of *Panax* species. *Plant. Med.*, 77: 182-187.

(Received for publication 12 May 2023)